I-1267

MASTER

CONSEQUENCES OF TOROIDAL EFFECTS IN LOWER HYBRID HEATING OF TOKAMAKS

BY

S. Bernabei and D.W. Ignat

JANUARY 19, 1982

PLASMA PHYSICS LABORATORY

PRINCETON UNIVERSITY
PRINCETON, NEW JERSEY

Consequences of Toroidal Effects in Lower Hybrid

Heating of Tokamaks

S. Bernabei and D.W. Ignat

Plasma Physics Laboratory, Princeton University

Princeton, New Jersey   08544   USA

The lower hybrid slow wave tends to follow magnetic field lines.
Therefore, a generalization of Snell's Law modifies the wave length along the
magnetic field as the wave moves inward from an exciter through regions of
varying magnetic field strength.   Predicting the consequences requires a
numerical treatment, which has been developed in recent years by several
authors.   This paper searches for some general statements on the problem by
analyzing many particular cases, without allowing for scattering, multiple
traverses of the plasma radius, and non-linear effects.   We find that the
range of parameters suitable for ion heating varies from that predicted by
simple estimates, and is dependent on launch position; and that electron
heating including current drive is best pursued with unidirectional launching
from a coupler at the top (or bottom) of the torus if the wave frequency is
close to linear mode conversion condition.

1. INTRODUCTION

Several recent calculations have shown the importance of toroidal effects in lower hybrid heating of tokamaks [1-6] by integrating the ray equations of geometrical optics [7,8].

$$\frac{d\underset{\sim}{r}}{dt} = - \frac{\nabla_{\underset{\sim}{k}} D(\underset{\sim}{r}, \underset{\sim}{k}, \omega)}{\partial D/\partial \omega} \, , \tag{1a}$$

$$\frac{d\underset{\sim}{k}}{dt} = + \frac{\nabla_{\underset{\sim}{r}} D(\underset{\sim}{r}, \underset{\sim}{k}, \omega)}{\partial D/\partial \omega} \, . \tag{1b}$$

The real part of dispersion relation in Eq. (1) is represented by $D(\underset{\sim}{r}, \underset{\sim}{k}, \omega)$, and took different but nearly equivalent forms in Refs. [1-6]. In Refs. [1,2,4,5,6], damping estimates were accumulated along the ray path according to electron and ion Landau damping terms from the imaginary part of the dispersion relation.

The results are consistent among the several investigations [1-6], and can be summarized as follows

(1) $k_{\parallel} = \underset{\sim}{k} \cdot \underset{\sim}{B} / | \underset{\sim}{B} |$ varies importantly along the wave trajectory for tokamak parameters (safety factor $\sim$ 3, aspect ratio $\sim$ 3).

(2) The initial dominant change in $|k_{\parallel}|$ is downward for waves moving to smaller major radius and upward for waves moving to larger major radius. The dominant decrease almost masks the increase associated with conservation of "toroidal" (which is not the same as "parallel") wave number. Changes of $k_{\parallel}$ after the initial change are unpredictable without a detailed computation.

(3) Regions of absorption for both electron and ion Landau damping vary considerably from the regions predicted from the dispersion relation and the original $k_\parallel$.

In this paper we draw general conclusions about the result of toroidal effect for lower hybrid heating of tokamak plasmas.

2. DISPERSION RELATION AND DAMPING TERMS

The dispersion relation written in terms of $k_\parallel^2$ and $k_\perp^2 = |\underset{\sim}{k}|^2 - k_\parallel^2$ is

$$D(\underset{\sim}{r}, \underset{\sim}{k}, \omega) = k_\perp^4 K_\perp + k_\perp^2 \left[(k_\parallel^2 - k_o^2 K_\perp)(K_\parallel + K_\perp) + k_o^2 K_{xy}^2 \right]$$

$$+ K_\parallel \left[(k_\parallel^2 - k_o^2 K_\perp)^2 - k_o^4 K_{xy}^2 \right] = 0 \ , \tag{2}$$

where

$$K_\perp = 1 + \frac{\omega_{pe}^2}{\omega_{ce}^2} + \sum_i \frac{\omega_{pi}^2}{\omega^2} - \alpha \, k_\perp^2 \ , \tag{3a}$$

$$\alpha = \frac{3}{4} \frac{\omega_{pe}^2}{\omega_{ce}^4} \frac{T_e}{m_e} + 3 \sum_i \frac{\omega_{pi}^2}{\omega^4} \frac{T_i}{m_i} \tag{3b}$$

$$K_\parallel = 1 - \frac{\omega_{pe}^2}{\omega^2} \left(1 + \frac{3k_\parallel^2}{\omega^2} \frac{T_e}{m_e} - \frac{k_\perp^2}{\omega_{ce}^2} \frac{T_e}{m_e} \right) \tag{4}$$

$$K_{xy} \approx \frac{\omega_{pe}^2}{\omega\,\omega_{ce}} \;, \tag{5}$$

$$k_o^2 = \omega^2/c^2 \;. \tag{6}$$

Here the notation is standard, with ω_p the plasma frequency, ω_c the cyclotron frequency, T the temperature, m the mass, and secondary subscripts denoting electrons (e) and ions (i). Equations (2)-(5) are derived from standard expansions of the dielectric plasma tensor [9]. Other temperature correction terms from K_{xy} and K_{yy}, K_{xz}, K_{yz} are not important for the present application.

Equation (2) is electromagnetic, and contains the slow wave (usual lower hybrid wave with the approximate dispersion relation $k_\perp^2 K_\perp + k_\parallel^2 K_\parallel = 0$) and the fast wave, as well as coupling between the two modes. It also contains the mode conversion [10] to warm plasma waves near resonance ($K_\perp = 0$).

An estimate for the wave energy decrease dE/dt, good only for the slow wave when the fast and slow waves are well separated, can be obtained from a perturbation analysis of the imaginary hot plasma terms [2],

$$\frac{1}{E}\frac{dE}{\omega dt} = -\frac{2\sqrt{\pi}\;k_\perp^2}{\omega^2 \partial D/\partial \omega^2} \left[k_\parallel^2 \frac{\omega_{pe}^2}{\omega^2} F\left(\chi_e\right) + k_\perp^2 \sum_i \frac{\omega_{pi}^2}{\omega^2} F\left(\gamma_i\right) \right] \tag{7}$$

where

$$F(\chi) = \chi^3 e^{-\chi^2}, \;\; \gamma_e = \frac{\omega^2}{2k_\parallel^2} \left(\frac{m_e}{T_e}\right) \;; \;\; \gamma_i = \frac{\omega^2}{2k_\perp^2} \left(\frac{m_i}{T_i}\right) \;. \tag{8}$$

3.   COORDINATE SYSTEM AND PLASMA MODEL

As in Refs. [2] and [6] we use toroidal co-ordinates (r,θ,ϕ), where r is minor radius, θ is poloidal angle, and ϕ is toroidal angle.   Wave numbers conjugate to the spatial co-ordinates are (k_r, m_θ, n_ϕ), so that

$$k_\parallel^2 = (m_\theta/r \; B_\theta + n_\phi/(R + r \; \cos\theta) \; B_\phi)^2/|\underset{\sim}{B}|^2 \; ,$$

$$k_\perp^2 = k_r^2 + (m_\theta/r \; B_\phi - n_\phi/(R + r \; \cos\theta) \; B_\theta)^2/|\underset{\sim}{B}|^2. \tag{9}$$

The field distribution is approximated by $\underset{\sim}{B} = (0,b(r), \; B_0)/[1 + (r/R)\cos\theta]$, $b(r) = \mu_0 I \; [1 - (1 - r^2/a^2)^{q(a)}]/(2\pi r)$, $T_{e,i}(r) = T_{e,i}(0) \; (1-r^2/a^2)^{1.4,2}$, $n_e = n_e(0) \; (1 - r^2/a^2)^p$. We have used parabolic density profiles (p = 1) and the more peaked squared parabola (p = 2). Results of the simpler straight cylindrical model are recovered by making major radius R large while reducing plasma current I in proportion so that q(a) is held constant.

4.   PARAMETER RANGE FOR ION HEATING

A wave near the lower hybrid frequency propagating into a plasma can encounter different fates: it can be damped partially or totally by ions, or by electrons, it can couple to the fast wave branch of the dispersion relation and propagate out toward the edge of the plasma or it can cross the plasma without any major effect.

For a given set of plasma parameters the final fate of the wave is determined by its wave number parallel to the magnetic field.

The toroidal geometry affects directly this parallel wave number, hence it determines the behavior of the wave.

Examples of wave trajectories were reported previously (2). Here we will try to represent in a compact way all possible outcomes of the propagation of slow waves as predicted by linear theory including the corrections caused by toroidicity. There is no simple way to predict if and where waves with a certain $k_\parallel$-spectrum are damped in a plasma, other than to compute a large number of cases varying the wave and plasma parameters.

The results can be summarized with the aid of a diagram where damping location is indicated as a function of density and launched parallel index of refraction while temperature, field, frequency and all profiles are assumed constant.

Figure 1 is one of such summaries when toroidal effects are ignored: B_o is 32 kG, $T_e(0) = 1.5$ keV, $T_i(0) = 0.8$ keV, $a = 40$ cm. The density profile is taken parabolic ($p = 1$) and is characterized by its peak value $n_e(0)$; r is the plasma radius in cm. To understand the figure consider a plasma with peak density $n_e(0) = 2.5 \times 10^{13}$ cm^{-3} which would be represented by a horizontal line intersecting the ordinate at 2.5. The figure shows that: waves launched with $1.0 \leq n_{\parallel 0}$ 1.25 couple to the fast wave; waves with $1.25 \leq n_{\parallel 0} \leq 2.75$ will be undamped; waves with $2.75 \leq n_{\parallel 0} \leq 3.75$ will be damped by ions in the inner 10 cm of the plasma; waves with $3.5 \leq n_{\parallel 0} \leq 4.4$ will be damped between 10 cm and 15 cm from the center; and, finally, waves with $n_{\parallel 0} \geq 4.4$ will be damped mostly by the electrons. As another example, a wave launched from the edge of the plasma with $n_{\parallel 0} = 3.75$ will be damped by the ions at r = 10 cm when the density is parabolic and peaked at $n_{eo} = 2.5 \times 10^{13}$ cm^{-3} and the other parameters are as chosen. The lower portion of the $n_{\parallel 0}$ spectrum is damped by the ions and the location of the damping depends on the density. The higher

portion of the $n_{\parallel 0}$ spectrum is damped by electrons at radial locations largely independent of the density. This latter result is to be expected since electron Landau damping is determined mostly by the electron temperature. While the line labeled $r = 0$ is an effective boundary between damping and no-damping situations, the line separating ion and electron damping shows the approximate parameters for which the wave is damped equally by ions and by electrons. This means that electron damping extends somewhat to the left of this line and the opposite for ion damping. It is interesting to note that this line would shift to the left as a result of increasing the plasma temperature since electron damping is more strongly dependent on temperature than is ion damping: the consequence is the well known fact that at higher temperatures ion damping is restricted to an increasingly narrow range of parameters.

The bands of damping are narrower near the center because the density profile is parabolic and the density variation per unit radius is smaller in the center.

Figure 2 shows the result of taking into account toroidal effects, parameters are as in Fig. 1 and the wave is launched from the equatorial plane with $R_0 = 135$ cm and $I = 500$ kA. The ion damping region is shifted toward higher values of $n_{\parallel 0}$ and the density range for damping is slightly compressed.

It is possible to show that these results are a direct consequence of toroidicity. In the absence of toroidal effects $k_{\parallel}$ is a constant and $k_{\perp}$ is immediately obtainable by the dispersion relation: it monotonically increases as the wave propagates toward higher density. In Fig. 3 ion damping becomes strong at the heavy solid line; electron damping becomes strong above the heavy dashed line. This figure assembles results of the ray tracing code, but it could have been produced from analytic formulas because of the simplicity of the cylindrical geometry.

In toroidal geometry $k_{\parallel}$ is no longer a constant and $k_{\perp}$ has to satisfy the dispersion relation with $k_{\parallel}$ varying from point to point. The result is shown in Fig. 4: the rays penetrate deeper into the plasma but their $k_{\perp}$ does not reach values for damping (darkline); furthermore, the rays tend to "fan out" in the $k_{\perp}$ - r space. Comparing the two figures (3 and 4) it is possible to see that the portion of $n_{\parallel}$ - spectrum which deposits energy in the inner half of the plasma in narrower in the case of toroidal geometry. As a consequence a relatively narrow $n_{\parallel}$ - spectrum is desirable for central heating, requiring thus many elements in the launching structure. It should be noted that as the plasma gets heated, the bands of Fig. 2 shift to lower values of $n_{\parallel}$ and n_e, requiring a way to shift the $n_{\parallel}$ - spectrum to the desired range.

One important characteristic of parameter space at densities too low to yield damping in Figures such as Fig. 2 is that the perpendicular phase velocity of the wave is higher than the thermal velocity, but not so high that there are no particles in the plasma with the resonant speed. This fact can account for ion tail production in experiments unaccompanied by measurable heating[12]. Figure 5 shows approximate contours of resonant ion energies $[E_i = m_i (\omega/k_{\perp})^2/2]$ in the region of Fig. 2 where no ion damping occurs in the formula derived from linear theory. Contours are shown in a region where resonant perpendicular energy is approximately independent of position.

The discussion so far referred to the situation when the waves are launched from the equatorial plane at the point of minimum toroidal field: for these waves $n_{\parallel}$ tends to decrease as they penetrate into the plasma and the effect is independent of the direction of propagation. That behavior is the same for trajectories propagating to the right and to the left of the launcher.

The situation is different when the coupler is placed on the top or on the bottom of the vacuum vessel: in these cases waves launched toward increasing magnetic field behave quite differently from waves launched in the opposite direction. Figure 6 shows, as a reference, the radial variation of $n_\parallel$ for wave launched with position and direction shown in the inset.

Of particular interest are waves launched in the direction labeled "C". A plot similar to those of Figs. 1 and 2 is shown in Fig. 7. By comparing Figs 2 and 7 it is seen that launching the wave from top or bottom increases the area of parameter space which gives central damping and reduces considerably the portion of the spectrum which couples to the fast wave; it should be noted again that this is true for waves launched in the direction "C" of Fig. 6. Since it is impractical to avoid launching some energy in the opposite direction ("B"), there will always be wave energy encountering a much more severe accessibility condition.

The difference between cylindrical and toroidal geometry is seen best in the electron damping since this damping depends directly on $n_\parallel$. Looking at Fig. 2 it is seen that practically no portion of the $n_\parallel$ – spectrum heats electrons in the inner half of the plasma column. The reason for this behavior is explained by looking at the radial evolution of $n_\parallel$ in relation to the damping condition, represented by the heavy line of Fig. 8: high values of $n_\parallel$ are damped near the surface, while lower values are undamped because of their reduction as they reach the central part of the plasma. Equatorial launching is then not favorable for electron heating and current drive, which is best pursued launching the wave from top (or bottom) unidirectionally. (See Fig. 7 and 9).

5. SUMMARY AND CONCLUSION

Ray tracing analysis of lower hybrid experiments requires the compilation of large numbers of cases. We have done this within the limitation of linear propagation and damping theory with the intent to provide a reference point for the analysis of experimental results. In conclusion the range of parameters for ion heating near the center of a toroidal plasma is shifted respect to what is expected from a cylindrical calculation, but not much narrower.

Electron heating near the center can be achieved by placing the launching structure at the top or bottom of the vessel. These situations are recommended also for current drive experiments.

REFERENCES

[1]   MAEKAWA, T., TERUMICHI, Y., and TANAKA, S., IEEE Trans. on Plasma
       Science, Vol. PS-8, 67 (1980).

[2]   IGNAT, D.W., Phys. Fluids, 24 (1981) 1110.

[3]   FEDEROV, V.I., Second Joint Grenoble-Varenna Symposium on Heating in
       Toroidal Plasmas, Como, Italy (1980).

[4]   BARANOV Yu. F., and FEDEROV, V.I., Nuclear Fusion 20 (1980) 1111.

[5]   SANTINI F., TONON, M., in Heating in Toroidal Plasma (Proc. Joint
       Varenna-Grenoble Int. Symposium 1978) Vol. 2 (1978) 415.

[6]   BONOLI, P.T., Proceedings of the Fourth Topical Conference on Radio
       Frequency Plasma Heating, Austin, Texas, 1981, paper C1.

[7]   WEINBERG, S., Phys. Rev. 126 (1962) 1899.

[8]   BERNSTEIN, I.B., Phys. Fluids 18 (1975) 320.

[9]   STIX, T.H., The Theory of Plasma Waves, McGraw-Hill, New York, 1962.

[10]   STIX, T.H., Phys. Rev. Lett. 15 (1965) 878.

[11]   EJIMA, S., et al., Bull. Am. Phys. Soc. 22 (1977) 1170.

[12]   BERNABEI, S. et al., Bull. Am. Phys. Soc. 26 (1981) 975.

FIGURE CAPTIONS

Fig. 1   Regions of total damping of the wave if toroidal effects are ignored.
Numerals refer to radii, as explained in the text. B_O = 32 kG, $T_e(0)$ = 1.5
keV, $T_i(0)$ = 0.8 keV, deuterium ions.

Fig. 2   Same as Fig. 1 with toroidal effects taken into account I_p = 500 kA, R_O =
135 cm.   The broken line to the left indicates the range of parameters
where the slow wave couples to the fast wave.

Fig. 3   Radial evolution of $k_\perp$ for various values of $n_{\parallel 0}$. It refers to Fig. 1 (no
toroidal effects) at $n_e(0)$ = 3 $\times$ 10^{13} cm^{-3}.   The dark line shows the value
of $k_\perp$ and the radial location where 10% of the damping occurs (solid line =
ion damping, broken line = electron damping).

Fig. 4   Same as Fig. 3 with toroidal effects included. $n_e(0)$ = 3 $\times$ 10^{13} cm^{-3}.

Fig. 5   Damping regions as in Fig. 2, showing the energy of the ions resonating
with the wave in the "non-damping" region.

Fig. 6   Radial evolution of $n_\parallel$ for four particular launching positions: B_O = 32 kG,
I_p = 500 kA, $T_e(0)$ = 1.5 keV, $T_i(0)$ = 0.8 keV, $n_e(0)$ = 1.5 $\times$ 10^{13} cm^{-3},
deuterium ions.

Fig. 7   Same as Fig. 2: launching position "B" of Fig. 6.

Fig. 8   Radial evolution of $n_\parallel$. The heavy line represents 10% damping, in the
broken lines the waves are completely damped: launching position "A".

Fig. 9   Same as Fig. 8: wave launched in the direction labeled "C" in Fig. 6.
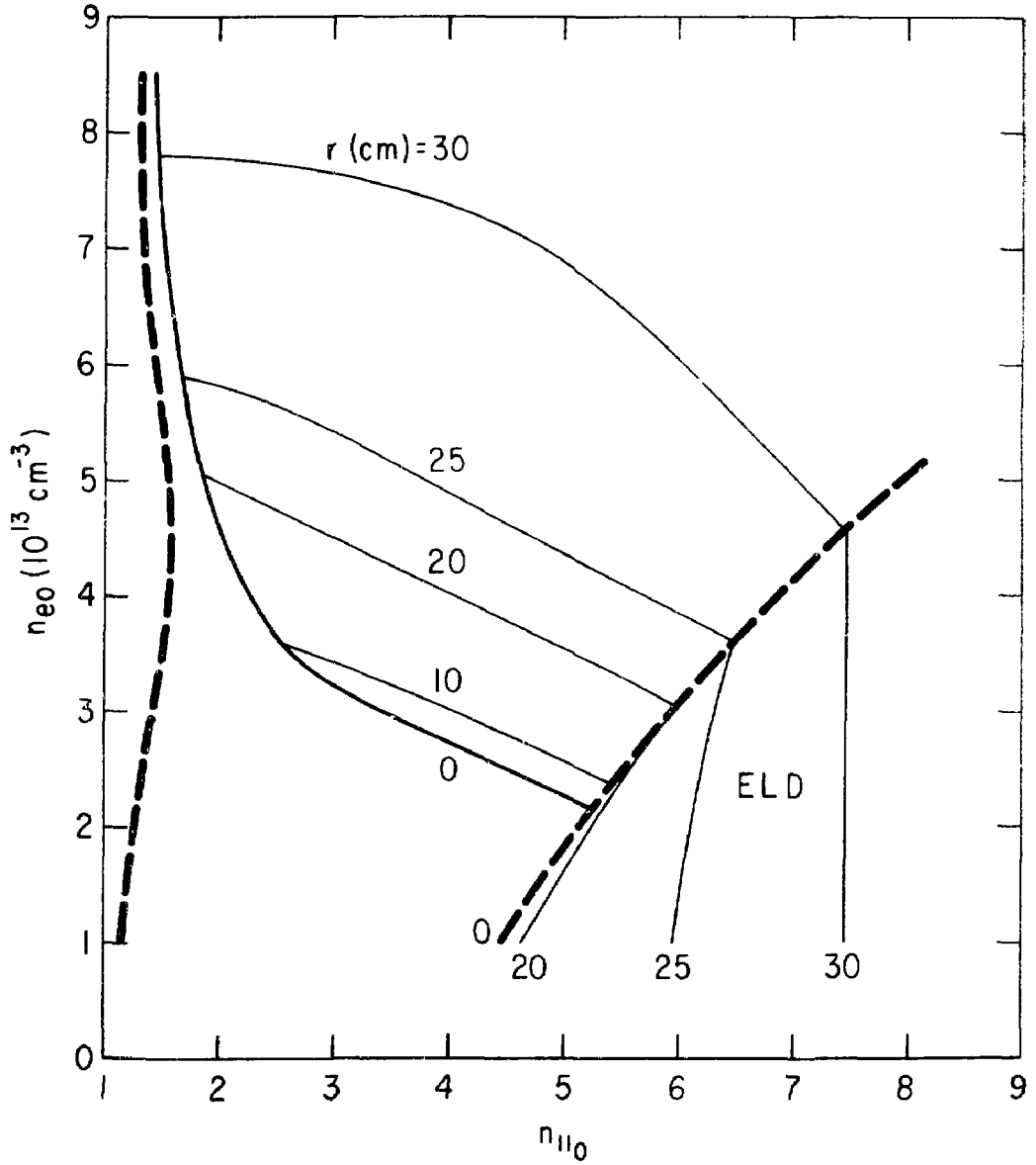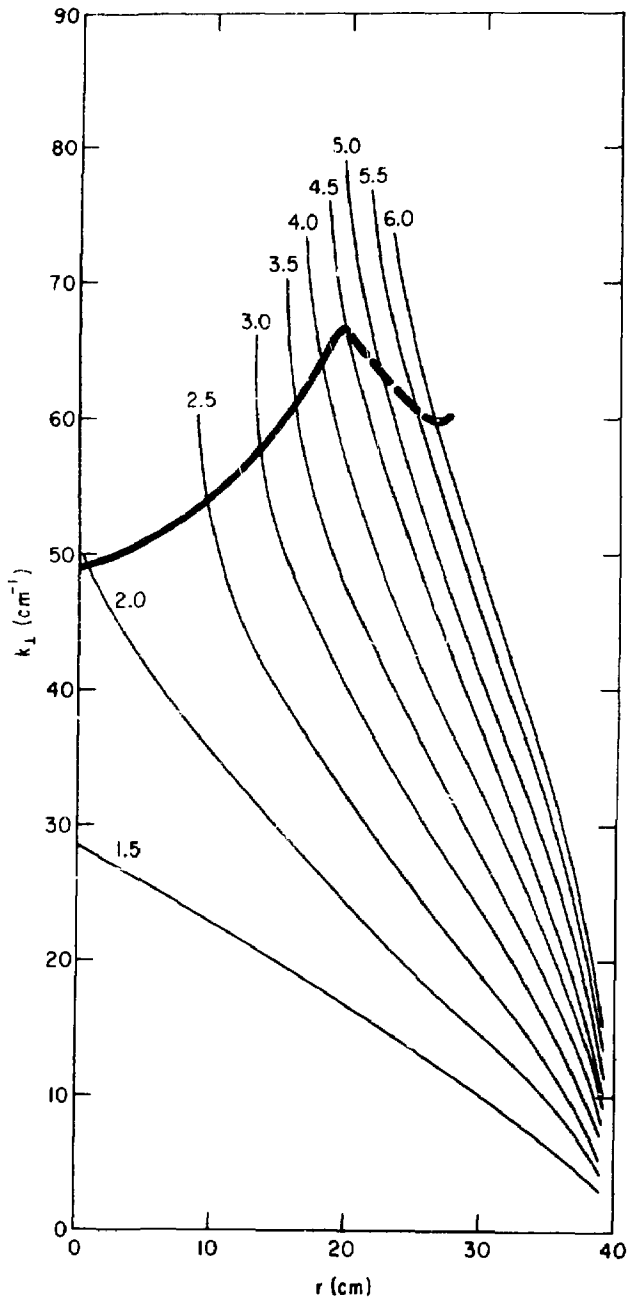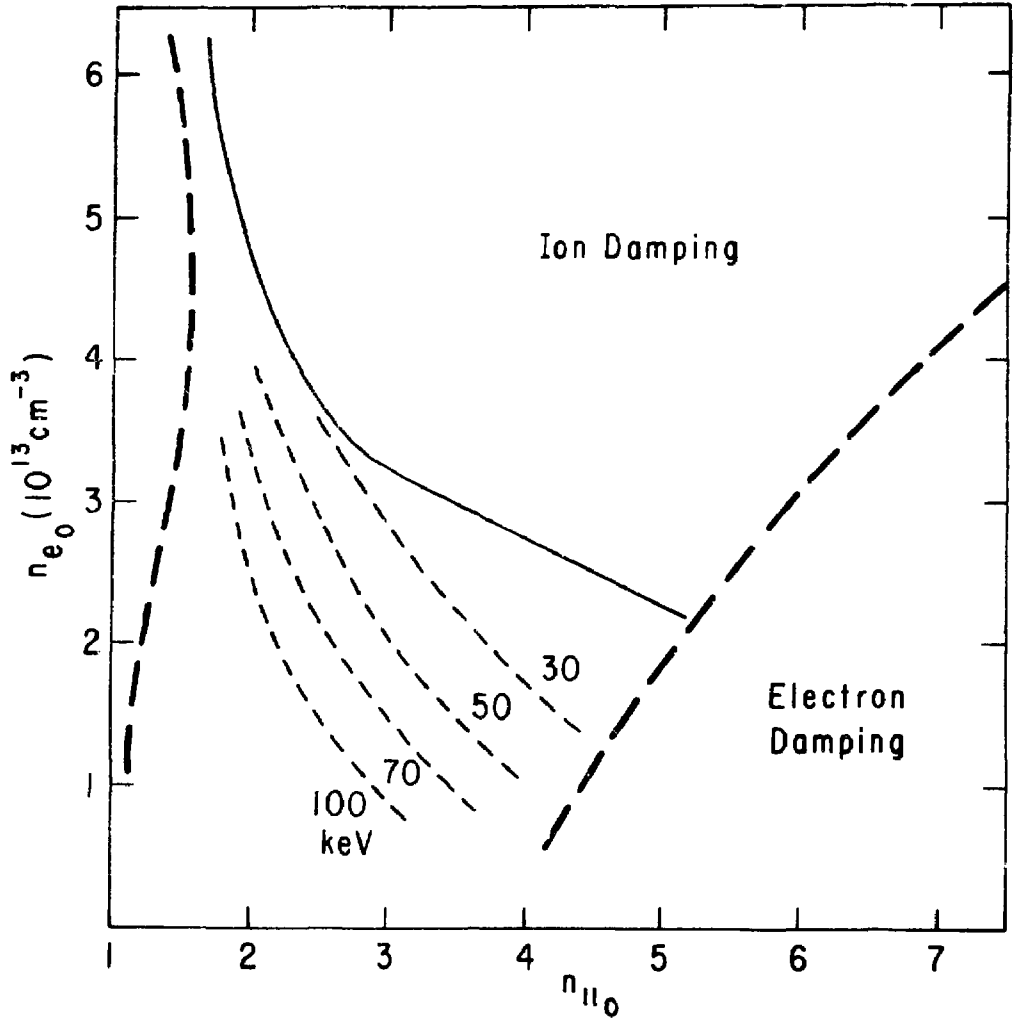
#81X1115

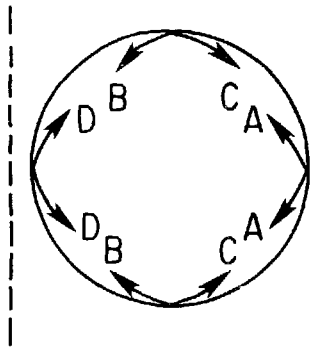

Fig. 1

#81X0748

Fig. 2

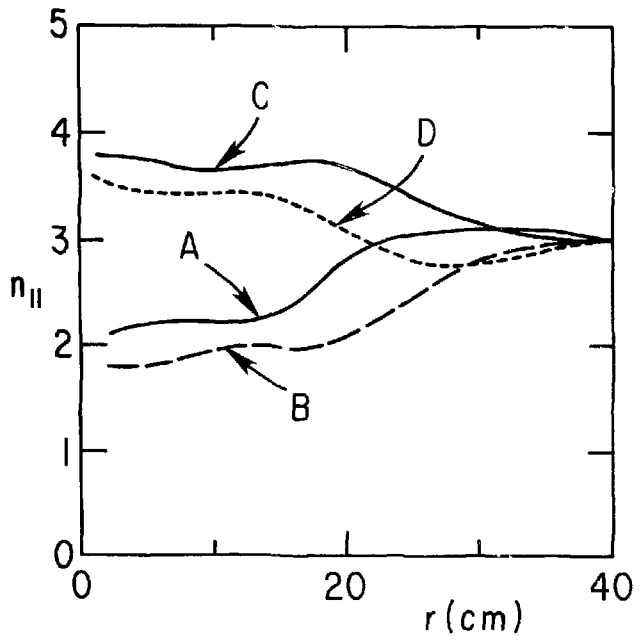# 81X0752

Fig. 3

#8IXIII4
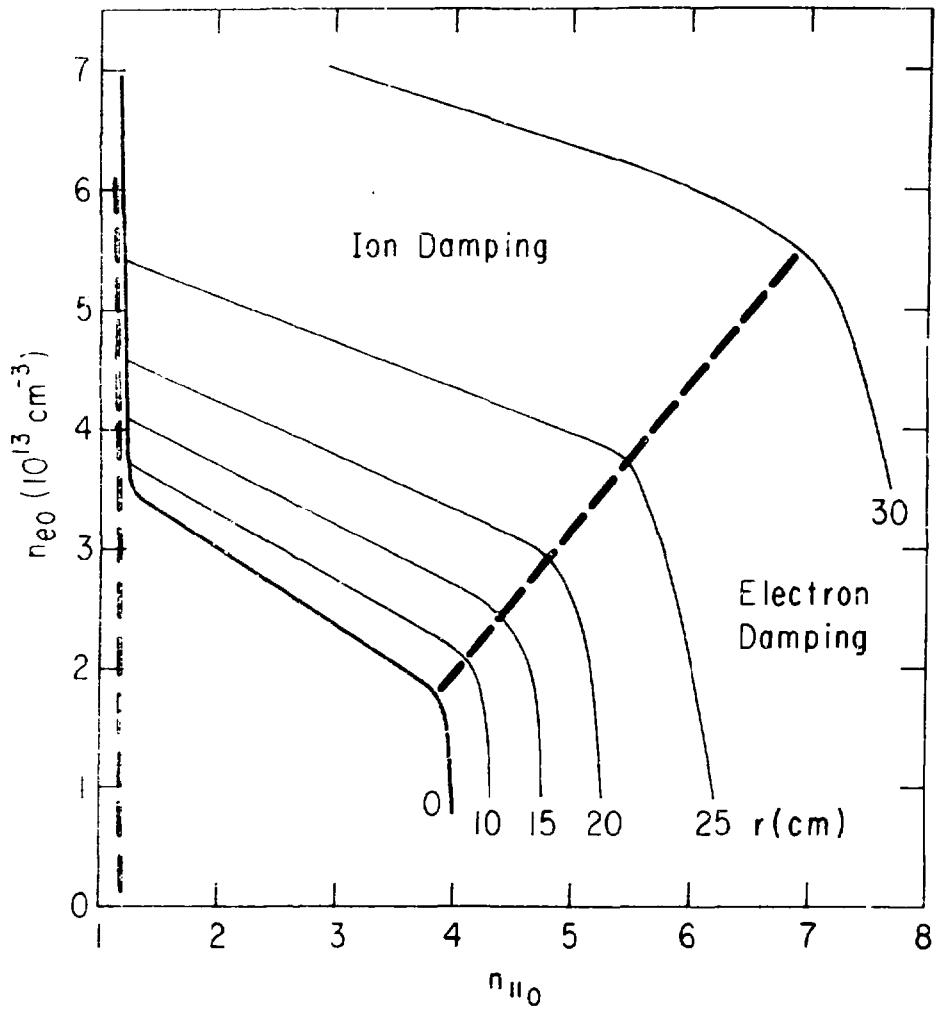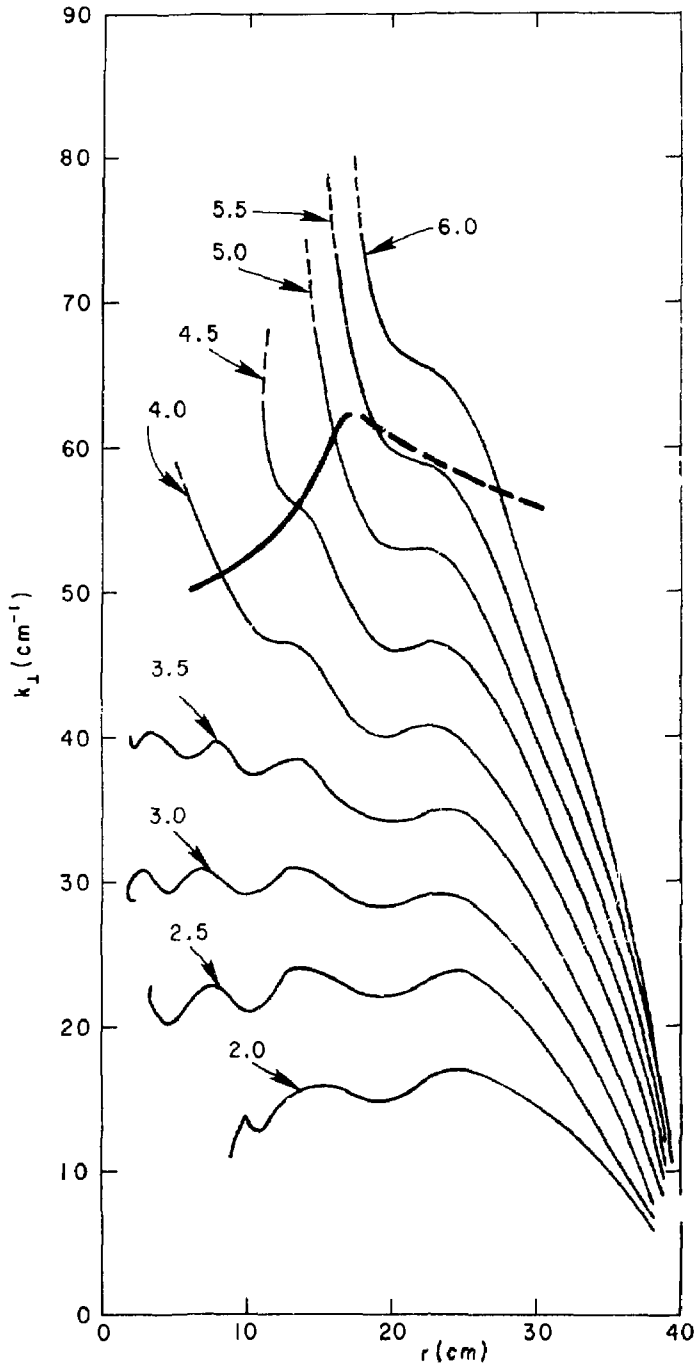
Fig. 4

Fig. 5

Fig. 6

81X1304
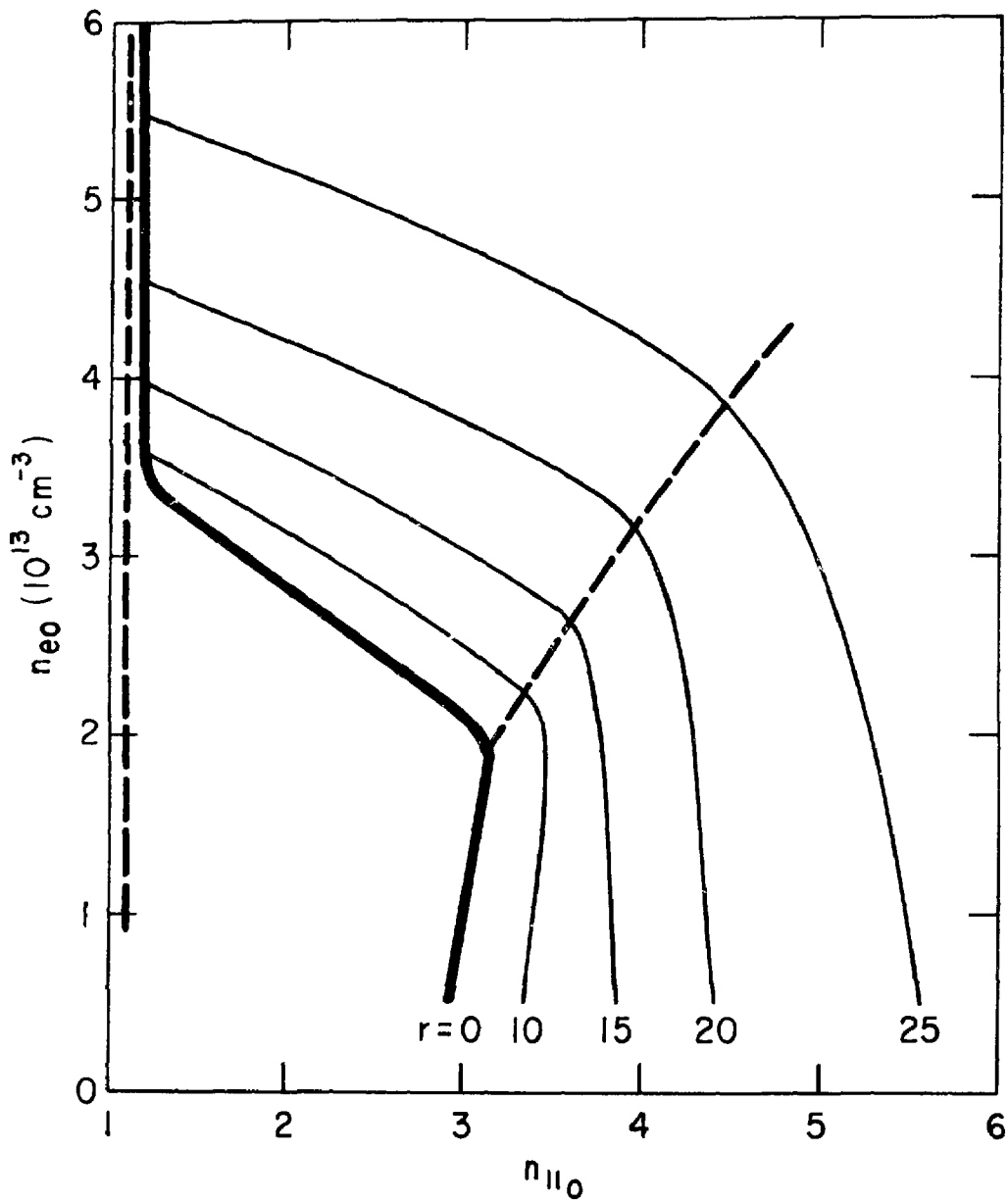
Fig. 7

#81X1113

Fig. 8
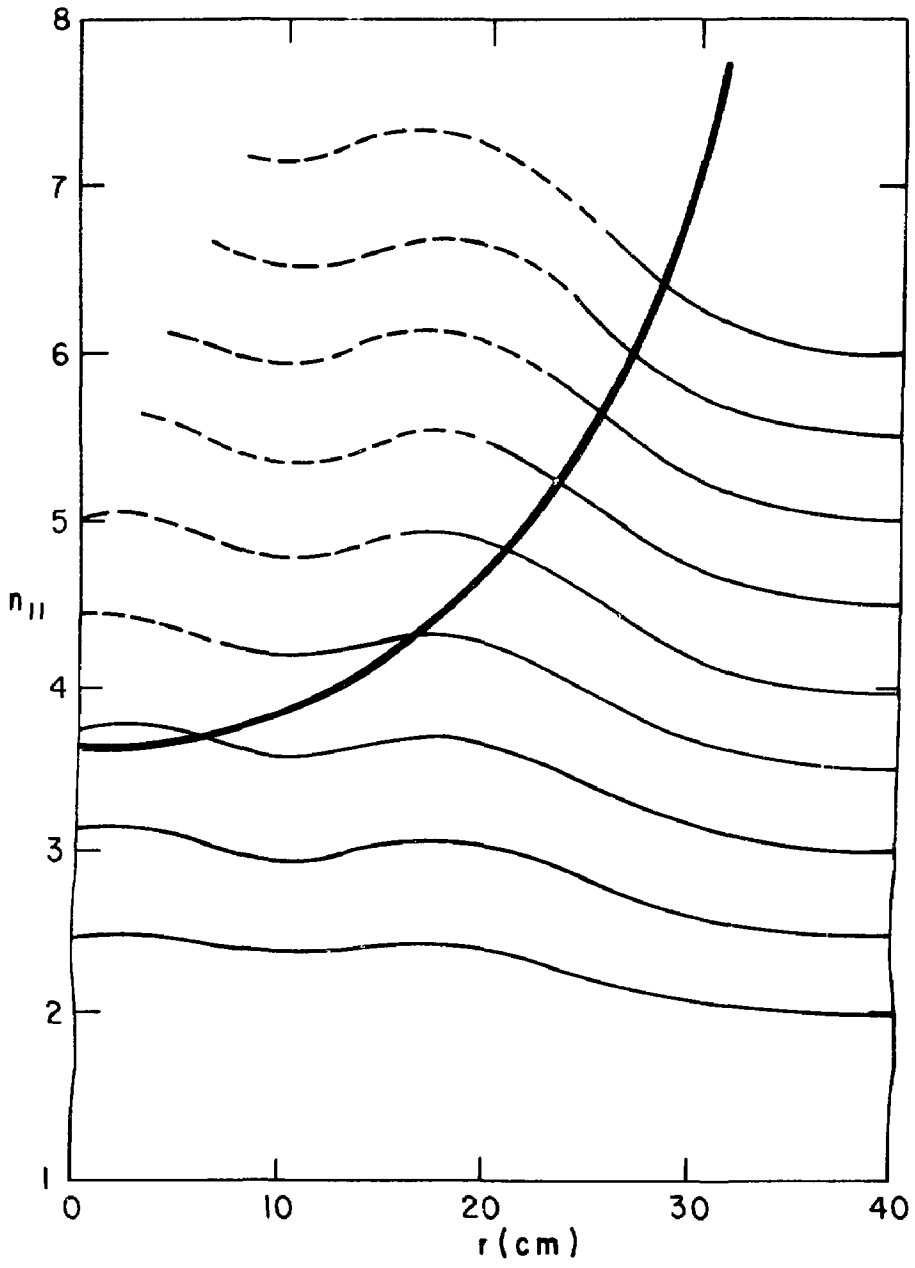
81 X 1 1 12

Fig. 9